Deformable Hybrid Model for Haptic Interaction

Máximo Mero
Dpto. de Matemáticas - FACYT
Universidad de Carabobo
Carabobo, Venezuela
mmero@uc.edu.ve

Antonio Susin
Dpt. Matemàtica Aplicada 1
Universitat Politècnica de Catalunya
Barcelona, Spain
toni.susin@upc.es

Abstract

In this paper a new hybrid deformable model for haptic interactions is presented. The main idea is to use a two layer deformable model for the virtual object which will be manipulated with a haptic tool by the user, when the external force is applied on the surface area. With this approach, deformation is modelled both using a continuous model, based on Finite Element Methods, and a discrete model defined by Mesh Free Methods.

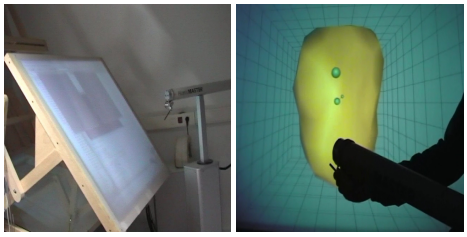

Figure 1: The workbench and phantom force-feedback device

1 Introduction

Simulating and animating 3D deformable objects in real time is essential to many interactive applications such as surgery simulators. One of the main characteristics of these simulations is the dynamic interaction between the deformable model and the possible external forces acting on it.

The dynamic behavior of our volumetric 3D deformable model is based on linear elastic mechanics. It is essentially based on techniques presented in computer graphics and mechanical engineering literature [8] , [10] and [3]. The works of J. O'Brien and J. Hodgins [7] and G. Debunne [4] are good references about the continuous deformation problem in terms of Finite Elements Method (FEM).

This model has been implemented in a workbench with a haptic device (as the Fokker Haptic Master) for interaction (see figure 1). Acting forces are computed from the reaction of the model when the user interacts with the virtual object.

The paper is organized as follows, sections 2 and 3 are devoted to introduce the FEM and MFM models respectively. In section 4 the hybrid model are defined. The dynamic of the virtual model is in section 5. Results and conclusion are in section 6 and 7 respectively. Results and conclusions are presented in the final sections.

2 Finite Element Formulation

The behavior of the molecules or particles of which the material is composed can be first modelled as continuous media. Let $u = (u_1, u_2, u_3)^T \in \mathbb{R}^3$ be a vector in $\mathbb{R}^3$ that denotes a location in the material coordinate frame.The deformation of the material is defined by the function $\mathbf{x}(u) = (x, y, z)$ that maps locations in the material coordinate frame to locations in world coordinates.

Green's strain tensor ε is used to measure the local deformation of the material [10].

$$\varepsilon_{ij} = \left(\frac{\partial \mathbf{x}}{\partial u_i} \cdot \frac{\partial \mathbf{x}}{\partial u_j} \right) - \delta_{ij}. \qquad (1)$$

Here δ_{ij} is the Kronecker's delta.

The stress and strain tensor are linked by

$$\sigma_{ij}^{(\varepsilon)} = \sum_{k=1}^{3} \lambda \varepsilon_{kk} + 2\mu\varepsilon_{ij}, \tag{2}$$

μ and λ are the Lamé coefficients, μ represents the rigidity of the material while λ measures its ability to preserve volume.

To improve realism, the following is considered

$$\nu_{ij} = \left(\frac{\partial \mathbf{x}}{\partial u_i} \cdot \frac{\partial \dot{\mathbf{x}}}{\partial u_j}\right) + \left(\frac{\partial \dot{\mathbf{x}}}{\partial u_i} \cdot \frac{\partial \mathbf{x}}{\partial u_j}\right), \tag{3}$$

where $\dot{\mathbf{x}} = \dfrac{\partial \mathbf{x}}{\partial t}$ is the velocity of a point. The viscous stress is

$$\sigma_{ij}^{(\nu)} = \sum_{k=1}^{3} \phi \nu_{kk} + 2\psi\nu_{ij}, \tag{4}$$

where ϕ and ψ control how fast the material looses kinetic energy.

The total stress tensor is obtained adding both the elastic and viscous stress $\sigma = \sigma^{(\varepsilon)} + \sigma^{(\nu)}$

By employing the Finite Element Method, linear tetrahedra elements will be used. The N_i is the shape function, associated to each vertex $\mathbf{x}_i$

$$N_i(x,y,z) = \beta_{i1}x + \beta_{i2}y + \beta_{i3}z + \beta_{i4}. \tag{5}$$

The matrix $\beta = (\beta_{ij})$ is defined from the material coordinates of the vertex. It is always a nonsingular matrix unless the associated tetrahedron is degenerated.

The internal force is computed for each element and is applied at their vertices

$$f_i^{(el)} = \frac{vol^{(el)}}{2} \sum_{j=1}^{4} \mathbf{x}_j \sum_{k=1}^{3} \sum_{l=1}^{3} \beta_{jl}\beta_{ik}\sigma_{kl}, \tag{6}$$

where $vol^{(el)}$ is the element volume.

3 Mesh Free Model

An approach for modelling deformation is to discretize the continuous material as a set of particles, or more precisely point samples, that carries out the material properties like density, strain and stress. Using this model a fixed mesh is not needed and because of that these methods are named *Mesh Free Method*, MFM (see [5],[9]).

The continuous function $\mathbf{x}(u)$ is approximated by

$$\mathbf{x}(u) \approx \int_{\Omega} \mathbf{x}(y) W(u-y,h)dy. \tag{7}$$

The displacements, velocity, and acceleration are interpolated using the kernel basis function W defined in (8). In the following, a short hand notation will be used: $W^i = W(u-u^i,h)$, $W^{ij} = W(u^i - u^j,h)$ and $\mathbf{x}^j = \mathbf{x}(u^j)$. The superscript j refers to the neighboring particle of i.

A potential function frequently used for SPH simulations (see [2], [6]) is the Lennard-Jones (LJ) given by

$$W(r_{ij}) = \varepsilon \left[\left(\frac{1}{r_{ij}}\right)^3 - \left(\frac{1}{r_{ij}}\right)\right] \tag{8}$$

where r_{ij} is the distance between two molecules i and j, and ε is the energy required to overcome the cohesion of molecules (see figure 2)

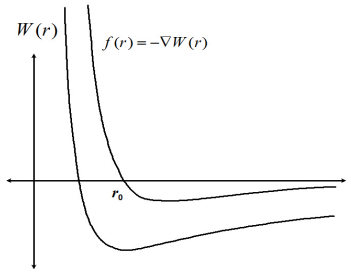

Figure 2: Lennard-Jones's potential function $W(r)$ and the associated force function $F(r)$

4 Hybrid Model

Suppose that the interpolation of $\mathbf{x}(u)$ in Ω, with $\Omega \in \mathbb{R}^3$ is built using both the finite element and mesh free method, the domain must include a set of $\{u^i\}_{i \in I_u^{N_i}}$ nodes with their associated base functions $N_i(u)$, which possess the information of the contributions of the finite element in $\mathbf{x}^f(u)$ as an approximation of the $\mathbf{x}(u)$ function. Therefore

$$\mathbf{x}^f(u) = \sum_{i \in I_u^{N_i}} \mathbf{x}(u^i) N_i(u). \tag{9}$$

A set of particles $\{u^j\}_{j\in I^h_{uj}}$ also exists with associated base functions $N^h_j(u)$, which possess the information of the contributions of the free mesh method in the approximation $\mathbf{x}^h$ of function $\mathbf{x}(u)$

$$\mathbf{x}^h(u) = \sum_{j\in I^h_u} \mathbf{x}(u^j) N^h_j(u). \tag{10}$$

The Ω domain is $\Omega = \mathrm{R1} \cup \mathrm{R2}$, where

$$\mathrm{R1} = \{u \in \Omega \quad / \quad \exists \quad i \in I^{N_i}; \quad N_i(u) \neq 0\},$$

and

$$\mathrm{R2} = \{u \in \Omega \quad / \quad \exists \quad j \in I^h; \quad N^h_j(u) \neq 0\},$$

Besides this, in the region where both interpolations have influence, $\widetilde{\Omega} = \mathrm{R1} \cap \mathrm{R2}$, a mixed interpolation must be defined

$$\mathbf{x}(u) \approx \mathbf{x}^f(u) + \mathbf{x}^h(u) \tag{11}$$

5 Dynamical Time Evolution

Once internal forces of the model are calculated, other possible external forces can be applied to compute the time evolution of the system. Essentially, Newtonian classical dynamics are considered

$$\dot{\mathbf{x}} = \mathbf{v}, \qquad \dot{\mathbf{v}} = \frac{F}{m}. \tag{12}$$

with the force F, mass m and the predicted acceleration are defined by

$$\begin{aligned} a &= \frac{F}{m} && \text{finite element method} \\ a &= \sum m^j \left(\frac{\sigma^j}{\rho^j \rho^i}\right) \frac{\partial W}{\partial u^j} && \text{SPH method} \end{aligned} \tag{13}$$

The Courant condition states that time increments have an upper maximum value to ensure stability,

$$\triangle t < h \sqrt{\frac{\rho}{2\lambda + \mu}}, \tag{14}$$

where h is the minimum of the distances between a node and its neighbors and ρ is the material's rest density.

6 Results

As a first approach for testing the finite element method, we build a simple model (ED0) consisting in two concentric ellipsoids. This model has been used as the interior of the virtual object described in the previous section. After some initial tuning, the final elasticity parameters and simulation time step are shown in table 1.

Our second test example is shown in figure (3) model (HM2) consisting in a heart model totally filled with tetrahedra. The obtained frame rate per second is about 29f/s. Although this result is adequate for realistic visual response effects, it is not sufficient for haptic interaction.

	λ	μ	Φ	Ψ	$\triangle t$
ED0	5.5	2.5	9.0e-5	9.0e-5	7.0e-3
HM1	5.0	2.0	9.0e-5	9.0e-5	7.0e-3
HM2	0.04	1.6e-3	1.0e-4	1.0e-4	7.5e-3

Table 1: Simulation parameter values used in our models.

The hybrid left ventricle model (HM1) presented in this paper is shown in figure (4). The region defined between the tetrahedra mesh and the exterior surface of the object does not have a uniform thickness. For this reason, with this model, the amount of particles that have to be activated for a haptic action varies between 50 and 600, being 200 the average amount of activated particles for the interaction. The total amount of particles initialized in the preprocess step in the region R2 is 27988. Using a personal computer with a Pentium IV and 2.8GHz processor, a suitable haptic frame rate is obtained, even in the worth case, with an interaction response of 330 frm/s.

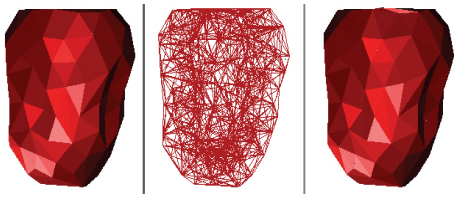

Figure 3: Model HM2. An actual left ventricle heart model filled with tetrahedra.

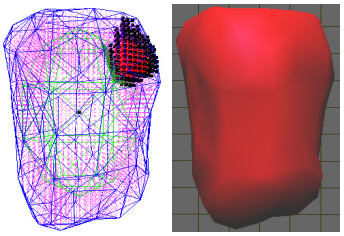

Figure 4: Model HM1. Internal deformable model of tetrahedra and activated particle region (left). Surface visualization at rest and after interaction (right).

7 Conclusions and Future Work

In this work we present a new deformable model suitable for haptic interaction.We have applied this methodology to the construction of a volumetric object adjusted to a human data set of the left ventricle.

This object is divided in two different domains for simulation. In the inner one, linear tetrahedra finite elements are used. A coarse mesh allows to move this biggest volumetric part in a very fast way. In the comprise volume between the previous one and the surface of the object, we have builded a particle zone simulated with a mesh free method (SPH).

The goal is to reconstruct the shape of the left ventricle of an actual patient from its SPECT captured data. As a first step, two meshed surfaces, corresponding to the external and internal walls of the left ventricle, are obtained.

We are working now in improving both, efficiency and deformation sensibility using different size partitions on the particles zone. Another research line can be to implement other type of mesh free methods like the Free Galerking Method to compare with the present SPH implementation [1].

8 Acknowledgments

This research is partially supported by a TIN-2004-08065-C02-01 CYCIT project. The first author is also supported by a Carabobo University (Venezuela) grant. The tetrahedra heart mesh corresponding to model 2 has been supplied by Enrique Escolano from CIMNE-UPC.

References

[1] A.Huerta and S.Fernández. Enrichment and coupling of the finite element and meshless methods. *International Journal for Numerical Methods in Engineering*, 48:1615 – 1636, 2000.

[2] B.Alder and T.Wainwright. Phase transition for a hard sphere system. *J. Chem. Phys*, 27:1208–1209, 1957.

[3] D.Terzopoulos. Regularization of inverse visual problems involving discontinuities. *IEEE Trans. Pattern Analysis and Machine Intelligence*, 8(4):413 – 424, 1986.

[4] G.Debunne, M.Dsbrun, M.Cani, and A.Barr. Dynamic real-time deformations using space and time adaptive sampling. *In SIGGRAPH 2001 Conference Proceedings*, 2001.

[5] J.Chen, C.Pan, C.Wu, and W.Liu. Reproducing kernel particle methods for large deformation analysis of no-linar. *Computer Methods in Applied Mechanics and Engineering*, 139:195 – 227, 1996.

[6] J.McCammon, B.Gelin, and M.Karpus. Dynamics of folded proteins. *Nature*, 267(1):585–590, 1977.

[7] J.O'Brien and J.Hodgins. Graphical models and animation of brittle fracture. *In SIGGRAPH'99 Conf. Proc.*, pages 137 – 146, 1999.

[8] R.Cool and D.Malkus. Concepts and applications of finite element analysis. In John Wiley and Sons., editors, *Concepts and applications of finite element analysis*. 1989.

[9] W.Liu, Y.Chen, S.Jun, J.Chen, T.Belytschko, C.Pan, R.Uras, and C.Chang. Overview and applications of reproducing kernel particle methods. *Archives of Computational methods in Engineering, State of the art Reviewa*, 3:3 – 80, 1996.

[10] Y.Fung. Linear elasticity. In Prentice Hall Inc., editor, *Foundations of Solid Mechanics*. Englewood Cliffs, N.J, 1965.